HHS Public Access

Author manuscript

Nat Med. Author manuscript; available in PMC 2013 November 01.

Published in final edited form as:

Nat Med. 2013 May ; 19(5): 586–594. doi:10.1038/nm.3150.

Cholesterol efflux in megakaryocyte progenitors suppresses platelet production and thrombocytosis

Andrew J. Murphy[1,#], **Nora Bijl**[1,#], **Laurent Yvan-Charvet**[1], **Carrie B. Welch**[1], **Neha Bhagwat**[2], **Adili Reheman**[3], **Yiming Wang**[3], **James A. Shaw**[4], **Ross L. Levine**[2], **Heyu Ni**[3], **Alan R. Tall**[1,*], and **Nan Wang**[1,*]

[1]Division of Molecular Medicine, Department of Medicine, Columbia University, New York, New York 10032, USA

[2]Human Oncology and Pathogenesis Program and Leukemia Service, Department of Medicine, Memorial Sloan-Kettering Cancer Center, New York, New York 10065, USA

[3]Canadian Blood Services and the Department of Laboratory Medicine and Pathobiology, St Michael's Hospital, University of Toronto, Toronto, Canada

[4]Department of Cardiovascular Medicine, Alfred Hospital/Baker IDI Heart and Diabetes Institute, Melbourne, Victoria, Australia

Abstract

Platelets play a key role in atherogenesis and its complications. Both hypercholesterolemia and increased platelet production promote athero-thrombosis; however, a potential link between altered cholesterol homeostasis and platelet production has not been explored. Transplantation of bone marrow (BM) deficient in ABCG4, a transporter of unknown function, into *Ldlr*$^{-/-}$ mice resulted in thrombocytosis, accelerated thrombosis and atherosclerosis. While not detected in lesions, *Abcg4* was highly expressed in BM megakaryocyte progenitors (MkP). *Abcg4*$^{-/-}$ MkPs displayed defective cholesterol efflux to HDL, increased cell surface levels of thrombopoietin (TPO) receptor (c-MPL) and enhanced proliferation. This appeared to reflect disruption of the negative feedback regulation of c-MPL levels and signaling by E3 ligase c-CBL and cholesterol-sensing LYN kinase. HDL infusions reduced platelet counts in *Ldlr*$^{-/-}$ mice and in a mouse model of myeloproliferative neoplasm, in a completely ABCG4-dependent fashion. HDL infusions may offer a novel approach to reducing athero-thrombotic events associated with increased platelet production.

Corresponding author: Dr. Nan Wang, P&S 8-401, Department of Medicine, Columbia University, 630 West 168th Street, New York, NY 10032, (212)342-1761, nw30@columbia.edu.

[#*]These authors contributed equally to this study.

AUTHOR CONTRIBUTIONS

A.J.M., N.B. and N.W. conceived the study, designed, performed and analyzed the experiments and wrote the manuscript. L.Y, C.B.W, N.B, A.R, Y.W, and J.A.S designed, performed and analyzed experiments. R.L.L and H.N. provided intellectual input and assisted with the preparation of the manuscript. A.R.T. conceived the study and contributed to writing the manuscript.

Supplementary information is available online.

INTRODUCTION

Athero-thrombotic events resulting in heart attack and stroke are the leading cause of morbidity and mortality globally[1]. Platelets are involved in multiple steps leading to athero-thrombosis, both in the promotion of atherosclerotic plaque growth and also in the formation of thrombus on ruptured or eroded plaques[2–5]. Increased numbers and activation of platelets both contribute to athero-thrombotic risk[6,7], and increased platelet production may underlie these processes[6,8]. A striking example of this occurs in myeloproliferative neoplasms such as myelofibrosis (MF) and essential thrombocytosis (ET), in which mutations in the thrombopoietin receptor (MPL) or its downstream signaling elements, lead to excessive production of megakaryocytes and thrombocytosis[9]. More generally, increased platelet production, denoted by increased platelet volume and increased numbers of circulating reticulated platelets, is a major risk factor for atherosclerotic cardiovascular disease, and may precipitate acute coronary syndromes[6].

Increased levels of LDL and decreased levels of HDL are also well known major risk factors for athero-thrombosis[10]. The athero-protective functions of HDL are thought to be mediated by its ability to promote cholesterol efflux from cells in the arterial wall, in a process that is facilitated by the ATP binding cassette transporters, ABCA1 and ABCG1[11]. While hypercholesterolemia has been associated with increased platelet production, the underlying mechanisms are unclear[12]. Moreover, potential mechanisms linking defective cholesterol efflux pathways to platelet production have not been explored.

The ATP binding cassette transporter ABCG4, which is highly homologous to ABCG1 promotes cholesterol efflux to HDL when overexpressed in cultured cells[13,14]. However, ABCG4 is not expressed in macrophage foam cells and *in vivo* functions and potential role in atherogenesis have remained enigmatic. *Abcg4* expression has been detected in the brain and in hematopoietic tissues such as fetal liver and BM[15,16]. In order to uncover a potential function of hematopoietic ABCG4, we have assessed hematopoietic functions and atherogenesis in a hypercholesterolemic mouse model of atherosclerosis.

RESULTS

Bone Marrow ABCG4 Deficiency Accelerates Atherosclerosis and Arterial Thrombosis

We assessed hematopoietic parameters and atherogenesis in a hypercholesterolemic mouse model of atherosclerosis, in which we reconstituted irradiated *Ldlr*$^{-/-}$ mice with BM from WTor *Abcg4*$^{-/-}$ mice. After feeding a high fat high cholesterol diet (WTD) for 12 weeks, atherosclerotic lesions were significantly increased in the aorta of *Ldlr*$^{-/-}$ recipient mice reconstituted with ABCG4-deficient BM cells (Fig. 1a). In contrast, the single deficiency of ABCG1 in the BM did not increase advanced atherosclerosis, consistent with previous studies[17,18]. Histological analysis of lesions showed typical, macrophage foam cell-rich atherosclerotic lesions, with no differences in morphology between groups (Supplementary Fig. 1a). The *Abcg4* knockout mice were created using a *lacZ* knock-in[14]. However, no *lacZ*-positive cells were detected in lesions of *Abcg4*$^{-/-}$ BM recipient mice (Fig. 1b). As a positive control, *lacZ*-positive cells indicating *Abcg1* expression in lesions were readily detected in the *Ldlr*$^{-/-}$ recipients reconstituted with *Abca1*$^{-/-}$*Abcg1*$^{-/-}$ BM. Plasma lipid

and lipoprotein levels were similar in WT or *Abcg4*$^{-/-}$ BM recipients (Supplementary Fig. 1b–d). The leukocyte, monocyte (Supplementary Fig. 1e, f), total lymphocyte, B- and T-cell counts (not shown) were also similar. Unexpectedly, the platelet count was 52% greater in *Abcg4*$^{-/-}$ BM recipient compared with WT recipients (Fig. 1c). Mild anemia and reticulocytosis were observed in the *Abcg4*$^{-/-}$ BM transplanted (BMT) *Ldlr*$^{-/-}$ recipient mice (Supplementary Fig. 1g, h).

Activated platelets contribute directly to atherogenesis[4], in part by promoting activation and adhesion of monocytes to arterial endothelium[3,4]. Platelet-neutrophil and platelet-Ly6-C^{hi} monocyte aggregates, were increased in hypercholesterolemic *Abcg4*$^{-/-}$ compared to WT BMT mice (Supplementary Fig. 1i). These aggregated leukocytes from the *Abcg4*$^{-/-}$ mice expressed higher levels of CD11b (MFI), a key cell adhesion molecule that facilitates adhesion to the endothelium[19] (Fig. 1d), indicating they were more activated. Depletion of platelets by injection of CD41 antibodies, which markedly reduced platelet count in the WT and *Abcg4*$^{-/-}$ BMT *Ldlr*$^{-/-}$mice (not shown), reduced aggregate numbers and leukocyte CD11b expression (Supplementary Fig. 1i and Fig. 1d). Platelet microparticles promote atherogenesis by facilitating chemokine deposition onto arterial endothelium and recruitment of monocytes to lesions[20]. The levels of platelet-derived microparticles were 3-fold higher in hypercholesterolemic *Abcg4*$^{-/-}$ than in WT BMT mice (Fig. 1e). Circulating reticulated platelets levels correlate directly with platelet reactivity[21] and are strongly associated with increased risk of myocardial infarction in humans[22]. There was also a significant increase in the percentage of reticulated platelets (Fig. 1f), consistent with increased platelet production and turnover[23]. These findings are consistent with previous studies in which infusions of activated platelets increased atherosclerotic lesion formation[4], and suggest that increased endogenous platelet production in *Abcg4*$^{-/-}$ BMT mice leads to accelerated atherogenesis.

Thrombocytosis and increased levels of reticulated platelets would also be expected to promote thrombosis. Mice are resistant to spontaneous thrombosis on atherosclerotic plaques. Thus, to assess thrombogenicity, we evaluated thrombus formation in whole blood using an *ex vivo* perfusion chamber model and showed a marked increase in *Abcg4*$^{-/-}$ platelet adhesion and aggregation to a collagen-coated surface under shear-flow conditions (Fig. 1g). We also examined arterial thrombosis *in vivo* using a carotid artery thrombosis model. Carotid artery occlusion by thrombus following $FeCl_3$ injury was significantly accelerated in *Abcg4*$^{-/-}$ BMT mice (Fig. 1h). Together, these findings indicate an increased propensity to thrombus formation in hypercholesterolemic mice with BM ABCG4 deficiency.

ABCG4 is selectively expressed in BM platelet progenitors

We first considered that ABCG4 might be acting in platelets to influence cholesterol efflux and platelet numbers. However, we did not detect *Abcg4* mRNA in WT platelets, or LacZ staining in platelets of *Abcg4*$^{-/-}$ mice (not shown). There was no alteration in platelet cholesterol efflux to HDL, or platelet cholesterol levels in *Abcg4*$^{-/-}$ *mice* (Supplementary Fig. 2a,b), indicating that ABCG4 is not acting in platelets to regulate circulating platelet levels and a mechanism distinct from those previously reported[24].

The phenotype of ABCG4 deficiency, with prominent thrombocytosis, increased reticulated platelets, mild anemia, increased platelet/leukocyte aggregates and increased platelet microparticles, resembles that of ET[25], a myeloproliferative neoplasm in which mutations in c-MPL or JAK2 in BM progenitors leads to excessive proliferation of platelet progenitors and increased platelet production[9,26]. Platelets are produced by megakaryocytes in the BM and spleen, and megakaryocytes are derived from megakaryocyte/erythrocyte progenitors (MEP). This suggested that ABCG4 might be expressed in BM platelet progenitors and involved in regulation of their proliferation and megakaryocytopoiesis. Following separation of BM hematopoietic cell populations by FACS (Supplementary Fig. 3), *Abcg4* mRNA was primarily detected in MEPs (Fig. 2a), with lower expression in the common myeloid progenitor (CMP) population. Very low or no *Abcg4* expression was observed in the other cell types (Fig. 2a). The restricted expression of *Abcg4* in MEPs contrasts with *Abca1* and *Abcg1* which are highly expressed in HSPCs but not in MEPs, even following induction with LXR activator treatment (Supplementary Fig. 4a,b). Recent studies have shown that the MEP population contains $CD41^+$ cells with megakaryocyte progenitor potential as well as $CD71^+$ cells with erythrocyte progenitor potential[27]. We further sorted the MEP population into $CD41^+/CD71^{lo}$, $CD41^{lo}/CD71^+$ or $CD41^{lo}/CD71^{lo}$ cell populations (Fig. 2b) and refer to $CD41^+/CD71^{lo}$ cells as megakaryocyte progenitors (MkP). High *Abcg4* expression was detected in MkP (Fig. 2c) and $CD41^{lo}/CD71^+$ cells (not shown) with lower expression in $CD41^{lo}/CD71^{lo}$ MEPs (Fig. 2c). To assess ABCG4 protein expression and localization in MkPs, immunofluorescence confocal microscopy was used. Specific ABCG4 staining was detected in wild type MkPs with anti-ABCG4 antibody but not in $Abcg4^{-/-}$ MkPs or WT MkPs stained with isotype-matched control antibody (Fig. 2d). Interestingly, ABCG4 staining partially co-localized with Golgi and, particularly trans-Golgi markers (Fig. 2e), while no co-localization with c-MPL (plasma membrane), Lamp2 (lysosome) or calnexin (endoplasmic reticulum) was detected (Supplementary Fig. 5 and not shown). Thus, Abcg4 is selectively expressed in the MEP and MkP populations, and ABCG4 appears to localize partly to the trans-Golgi.

ABCG4 Deficiency Increases Proliferation of MEP and MkPs and Promotes Megakaryopoiesis

There was a significant increase in the percentage in BM of MkPs and $CD41^{lo}/CD71^{lo}$ MEPs, but not HSPCs or CMPs, in hypercholesterolemic $Abcg4^{-/-}$ BM recipients (Fig. 2f). $CD41^{lo}/CD71^+$ erythrocyte progenitors were also significantly increased (not shown). The mRNA levels of GATA1, PU.1, EKLF and Fli1, transcription factors known to have critical roles in regulation of MEP, MkP and erythrocyte progenitor cell proliferation and differentiation, were similar in $Abcg4^{-/-}$ $CD41^{lo}/CD71^{lo}$ MEP, $CD41^+/CD71^{lo}$ MkP and $CD41^{lo}/CD71^+$ erythrocyte progenitors (not shown), suggesting that there was no marked alteration in lineage choice of $Abcg4^{-/-}$hematopoietic cells.

TPO is the most important growth factor regulating megakaryocyte/platelet lineage development *in vivo*[28]. We did not observe any changes in plasma TPO levels of $Abcg4^{-/-}$ BMT mice (Supplementary Fig. 6a). However, we discovered increased levels of c-MPL on the surface of $Abcg4^{-/-}$ MkPs and $CD41^{lo}/CD71^{lo}$ MEPs (Fig. 2g), but not megakaryocytes or platelets (Supplementary Fig. 6b,c). This is consistent with *Abcg4* expression profiles and

the hypothesis that increased MkP proliferation is the underlying mechanism of thrombocytosis. Indeed, there was increased EdU incorporation into DNA in MEPs from *Abcg4*$^{-/-}$ mice (Supplementary Fig. 6d). Colony formation assays showed a 2.5-fold increase in the number of megakaryocyte colonies developing in ABCG4 deficient BM compared to WT in response to TPO (Fig. 2h). Moreover, the number of megakaryocytes was increased in the BM and spleen of *Abcg4*$^{-/-}$ BM *Ldlr*$^{-/-}$ recipient mice (Supplementary Fig. 7a,b).

Increased Platelet Production in Response to Thrombopoietin in *Abcg4*$^{-/-}$ Mice

Platelet counts are tightly regulated by a negative feedback mechanism in which c-MPL at the surface of megakaryocytes and platelets serves as a clearance sink for TPO, and thus limits the increase in platelet count that results from increased TPO/c-MPL signaling in BM cells[28,29]. Giving exogenous TPO to animals may overwhelm the negative feedback regulatory mechanism, uncovering effects of increased c-MPL activity[30]. To test our hypothesis that ABCG4 deficiency in MEPs and MkPs results in increased cell surface levels of c-MPL, increasing sensitivity of cells to TPO and enhancing platelet production, we administered TPO to WT and *Abcg4*$^{-/-}$ mice. The increase in platelets was much more pronounced in *Abcg4*$^{-/-}$ mice (2.1-fold) compared to WT mice (1.4 fold) (Fig. 2i). These results indicate that ABCG4 deficiency renders the mice more responsive to TPO *in vivo*, consistent with increased c-MPL levels on MkPs as the mechanism underlying increased platelet production and levels in *Abcg4*$^{-/-}$ mice.

ABCG4 Promotes Cholesterol Efflux from MkPs to HDL and Modulates MkP Proliferation by Regulation of Membrane Cholesterol Content

We next sought to elucidate potential mechanisms linking ABCG4 deficiency to increased c-MPL and proliferation and expansion of MkPs. We first examined cellular cholesterol efflux from the WT or *Abcg4*$^{-/-}$ MkPs, using a novel fluorescent cholesterol analog (BODIPY-cholesterol) based flow cytometry assay. ABCG4 deficiency was associated with reduced cholesterol efflux to rHDL in *Abcg4*$^{-/-}$ MkPs (Fig. 3a). BODIPY-cholesterol levels in *Abcg4*$^{-/-}$ MkPs were also significantly increased (Fig. 3b). These findings could indicate defective cholesterol efflux via ABCG4 or that membranes of *Abcg4*$^{-/-}$ cells have a higher affinity/capacity for cholesterol. A significant portion of the BODIPY-cholesterol that accumulated in *Abcg4*$^{-/-}$ MkPs appeared to be in plasma membrane (Fig. 3c). Free cholesterol content as assessed by filipin staining was also substantially increased in the plasma membrane of *Abcg4*$^{-/-}$ MkPs (Fig. 3d). Cholesterol accumulation is known to suppress the expression of cholesterol-responsive genes[31]. Accordingly, expression of *Ldlr* and *Hmgcs1* was significantly decreased in *Abcg4*$^{-/-}$ relative to the WT MEPs but not in GMPs which do not express *Abcg4* (Supplementary Fig. 8a,b). Thus, even though localized to the Golgi (Fig. 2e), ABCG4 deficiency resulted in defective cholesterol efflux to HDL and an increase in cell cholesterol content including in the plasma membrane, consistent with studies suggesting segregation of sterol-rich plasma membrane domains in the trans-Golgi[32].

To see if increases in cellular cholesterol content could recapitulate the effects of ABCG4 deficiency, we loaded cells with cholesterol/cyclodextrin complexes (CD/Chol). This led to

increased WT MkP proliferation paralleling increases in cell surface c-MPL levels (Fig. 3e,f). When cells were treated with cyclodextrin (CD) to remove cellular cholesterol, proliferation and cell surface levels of c-MPL were significantly reduced to a similar level in both WT and *Abcg4*$^{-/-}$MkPs (fig. 3e,f). While rHDL significantly reduced WT MkP proliferation and cell surface c-MPL, it had no effect in *Abcg4*$^{-/-}$ MkPs, consistent with cholesterol efflux data (Fig. 3a). In addition, removal of cellular cholesterol by CD reversed the increase in megakaryocyte colonies associated with ABCG4 deficiency (Supplementary Fig. 8c). These findings suggest that ABCG4 acts to modulate MkP cell surface c-MPL levels and cell proliferation by regulation of membrane cholesterol content.

Decreased c-CBL-mediated down-regulation of TPO receptor in *Abcg4*$^{-/-}$ MkPs

We next sought to elucidate mechanisms linking changes in cellular cholesterol levels to altered c-MPL expression in MkPs. Previous studies have shown that TPO binding to its receptor (c-MPL) results in activation of a negative feedback loop in which c-CBL-mediated ubiquitinylation leads to receptor internalization and/or degradation[33]. c-CBL phosphorylation in response to the activation of growth factor receptors is required to mediate negative feedback regulation[34]. We assessed whether such negative feedback regulation is defective in *Abcg4*$^{-/-}$ MkPs. There was dramatic blunting of c-CBL tyrosine phosphorylation in response to TPO treatment in *Abcg4*$^{-/-}$MkPs compared to WT cells (Fig. 4a) while total c-CBL was unchanged (not shown). Treatment of WT MkPs with a proteasome inhibitor MG_{132} increased c-MPL to a similar level in WT and *Abcg4*$^{-/-}$ cells (Fig. 4b), consistent with a ubiquitination/proteasomal degradation mechanism. Cholesterol loading by CD/Chol reduced c-CBL phosphorylation, while removal of cellular cholesterol by CD increased c-CBL phosphorylation in WT and *Abcg4*$^{-/-}$ MkPs (Fig. 4c). Whereas phosphorylated c-CBL was increased in WT MkPs by rHDL, rHDL failed to alter c-CBL phosphorylation in *Abcg4*$^{-/-}$ MkPs (Fig. 4c), consistent with failure of rHDL to modulate c-MPL levels and cell proliferation of *Abcg4*$^{-/-}$ MkPs. These findings suggest that impaired cholesterol efflux in *Abcg4*$^{-/-}$ MkPs results in defective c-CBL-mediated feedback down-regulation of c-MPL by TPO.

LYN kinase acts upstream of c-CBL to modulate cholesterol-mediated proliferative responses

The kinase catalyzing c-CBL tyrosine phosphorylation in response to TPO is not known. SRC family kinases (SFK) such as LYN, FYN and c-SRC are known to phosphorylate tyrosine residues of c-CBL[35] leading to its activation and SFK inhibitors were shown to increase cell surface c-MPL levels via undefined mechanisms[28]. We hypothesized that the activity of SFK is decreased in *Abcg4*$^{-/-}$ MkPs, leading to decreased c-CBL phosphorylation. Consistent with this suggestion, treatment with SU6656, an inhibitor of LYN, FYN and c-SRC[36], markedly decreased c-CBL phosphorylation, increased cell surface c-MPL and abolished the difference in response to TPO in WT and *Abcg4*$^{-/-}$ MkPs (Fig. 4d,e). TPO activation of c-MPL increases the kinase activity of LYN and FYN but not other SFK[37]. LYN kinase is palmitoylated, membrane-associated and its activity is increased by decreased membrane cholesterol content[38]. Interestingly, *Lyn*$^{-/-}$ mice display increased megakaryocytopoiesis with mild thrombocytosis[39] and mild anemia with reticulocytosis[40], phenotypes that bear a striking resemblance to that of *Abcg4*$^{-/-}$ mice.

Thus, we hypothesized that LYN might be the dominant tyrosine kinase catalyzing c-CBL tyrosine phosphorylation in response to TPO. TPO-treated *Lyn*$^{-/-}$ MkPs showed decreased c-CBL phosphorylation and increased cell surface c-MPL (Fig. 4f,g) and cell proliferation (Fig. 4h), demonstrating a key role of LYN in regulation of tyrosine phosphorylation of c-CBL and MkP proliferation in response to TPO. Cholesterol loading by CD/Chol decreased c-CBL phosphorylation, increased c-MPL levels and enhanced cell proliferation in WT MkPs but had no effect in *Lyn*$^{-/-}$ MkPs (Fig. 4f–h). Treatments with either CD or rHDL to induce cholesterol efflux decreased proliferation of WT MkPs. In contrast, *Lyn*$^{-/-}$ MkPs showed increased proliferation that was completely unresponsive to either cholesterol loading or depletion conditions (Fig. 4h). These findings indicate an essential role of LYN Kinase in mediating the effects of cholesterol loading and unloading on c-CBL phosphorylation and TPO-mediated changes in c-MPL and MkP proliferation.

Lyn Kinase Activator Tolimidone Reduces c-MPL Levels on *Abcg4*$^{-/-}$ MkPs

We further assessed the possible involvement of LYN in negative regulation of MkP surface c-MPL levels by pharmacological activation of LYN. Treatment of BM cells from the hypercholesterolemic *Ldlr*$^{-/-}$ recipient mice with Tolimidone, a compound which selectively increases LYN kinase activity *in vivo* [41], reduced cell surface c-MPL levels in WT and *Abcg4*$^{-/-}$MkPs (Fig. 4i), and completely reversed the increased cell surface c-MPL levels in *Abcg4*$^{-/-}$MkPs from normocholesterolemic mice (Supplementary Fig. 9). Together the observations suggest that LYN kinase acts as a sensor of excessive membrane cholesterol accumulation, leading to decreased c-CBL mediated down-regulation of c-MPL by TPO.

We assessed known TPO-mediated signaling pathways that could potentially be activated in *Abcg4*$^{-/-}$ MkPs. Both basal and TPO-stimulated p-ERK1/2 and p-AKT levels were significantly higher in *Abcg4*$^{-/-}$ compared to WT MkPs; p-STAT5 levels were also non-significantly increased (Fig. 4j). This pattern is similar to that seen with LYN deficiency[39]. These findings suggest that effects of cholesterol loading and unloading on c-CBL phosphorylation, c-MPL levels and MkP proliferation may be mediated through LYN.

HDL Decreases Proliferation of MkPs and Reduces Platelet Count in an ABCG4-dependent Fashion

To test if HDL reduces MkP proliferation and platelet counts *in vivo*, we infused a preparation of reconstituted HDL (rHDL) that has been previously shown to reduce coronary atheroma volume in humans[42], into WTD-fed *Ldlr*$^{-/-}$ mice with or without ABCG4 deficiency. rHDL but not saline infusion significantly decreased platelet counts by ~30% in the mice expressing ABCG4 (Fig. 5a). Remarkably, rHDL had no effect in *Abcg4*$^{-/-}$ mice. Effects on blood platelets paralleled decreased c-MPL levels on MkPs, decreased numbers and proliferation of MkPs as well as decreased megakaryocyte counts in spleen and bone marrow in rHDL-infused *Abcg4*$^{+/+}$ mice while there was no effect of rHDL in *Abcg4*$^{-/-}$ mice (Fig. 5b,c and Supplementary Fig. 10a–c). These findings demonstrate an essential role of ABCG4 in mediating the ability of rHDL to reduce MkP proliferation and the platelet count.

We further explored the therapeutic potential for rHDL to reduce platelet counts in a mouse model of MF and ET, involving retroviral transduction of BM cells with an activating mutant form of MPL(W515L) found in human MPNs[26,43]. Such MPL mutations are found in a subset of patients with MF (~10%) and ET (~4–5%), and cause proliferation of MEPs, megakaryocyte expansion and thrombocytosis[9,26]. The activity of this mutant form of MPL requires cell surface localization[44], and since cell surface c-MPL level was increased in *Abcg4*$^{-/-}$ mice (Fig. 2g), this suggested that its activity might be enhanced by ABCG4 deficiency. Indeed, compared to WT mice, thrombocytosis developed more rapidly and was more pronounced in *Abcg4*$^{-/-}$ mice transduced with *Mpl*^{W515L} (Fig. 5d). While rHDL infusions effectively reversed thrombocytosis in WT mice expressing MPL(W515L), similar treatments had no effect on the platelet count in *Abcg4*$^{-/-}$ mice expressing MPL(W515L). Analysis of data obtained from a previously reported study involving patients with peripheral vascular disease[45], revealed that infusion of rHDL but not placebo was associated with a significant reduction of platelet counts (Fig. 5e); when normalized to baseline platelet values, the change was still significantly different between the groups (Fig. 5f). Importantly, the reduction of platelets in this study was moderate and the platelet count was maintained in the normal range (Fig. 5e).

Together these findings suggest that HDL and ABCG4 promote cholesterol efflux from MkPs and thus facilitate the negative feedback regulation of c-MPL by TPO in MkPs. (Fig. 5g). LYN kinase may act as a membrane cholesterol sensor, acting upstream of c-CBL to modulate its down-regulation of c-MPL.

DISCUSSION

Our findings show that defective cholesterol homeostasis in progenitor cells promotes megakaryocyte formation, platelet overproduction, arterial thrombosis and atherogenesis. Increased membrane cholesterol levels in megakaryocyte progenitors leads to increased levels and signaling of the TPO receptor. ABCG4 is highly expressed in MkPs and its deficiency leads to cholesterol accumulation, MkP proliferation and increased platelet production. The ability of rHDL to suppress MEP/MkP proliferation and platelet counts *in vivo* was completely dependent on ABCG4, likely reflecting the cell type restricted pattern of expression of cholesterol efflux promoting ABC transporters. Therapeutic interventions such as rHDL infusions have the potential to reverse excessive megakaryocytopoiesis in states of platelet overproduction, such as may occur in MPNs.

The idea that cellular sterol metabolism is intimately connected to proliferative responses is longstanding[46]. The requirement for new membrane synthesis during cell proliferation leads to activation of cholesterol biosynthesis involving cleavage of SREBP-2 and transcriptional induction of cholesterol biosynthetic genes[47]. Recent studies have linked control of cell proliferation to cholesterol efflux pathways mediated by ABCA1 and/or ABCG1[48–51]. However, specific molecular mechanisms linking cellular cholesterol accumulation to altered growth factor receptor signaling have not been defined. Our hypothesis that this involves LYN kinase is supported by previous studies showing that LYN kinase activity is modulated by altered membrane cholesterol[38]. LYN is palmitoylated and palmitoylation defective LYN shows decreased association with cholesterol-rich membranes but increased

ability to mediate tyrosine phosphorylation of immunoglobulin receptors[52]. Infusions of cholesterol-poor rHDL were associated with a reduction in platelet counts in a small study involving patients undergoing treatment for peripheral vascular disease, suggesting potential human relevance of our findings. Moreover, in a recent human GWAS SNPS in or near the *c-CBL* gene were associated with platelet counts[53]. Interestingly, *ABCG4* is in tight linkage disequilibrium with c-CBL, and SNPS associated with platelet counts could equally be influencing expression of *c-CBL* and/or *ABCG4*[53]. Our findings suggest a potential mechanism linking expression of *ABCG4* to the regulation of platelet counts, involving defective c-CBL mediated feedback regulation of c-MPL, and thus support the concept that these genes act in megakaryocytes or their progenitors to regulate platelet production[53].

There is tremendous interest in the development of new therapies that increase plasma HDL levels as potential treatments for atherosclerotic cardiovascular disease. This has proven challenging, as highlighted by the recent failure in clinical trials of treatments that increase HDL levels, such as the CETP inhibitors torcetrapib and dalcetrapib, and ER-niacin[54,55]. However, approaches that actively increase the flux of cholesterol from macrophages and other cells remain promising treatments to reduce coronary atherosclerosis[42,56]. Our study suggests that suppression of MEP and MkP proliferation and thrombocytosis may represent novel benefits of such treatments.

Currently, thrombocytosis in ET and MF is treated with low dose aspirin, and high-risk ET patients (age>60, or prior thrombotic event) are treated with genotoxic agents such as hydroxyurea[57]. There remains a need for novel therapies for MF patients given their poor overall outcome and limited therapeutic options[58]. Our findings suggest that rHDL infusions may specifically reverse MPL-dependent MEP proliferation and aberrant megakaryopoiesis underlying thrombocytosis in ET and MF. Moreover, increased platelet production is a cardiovascular risk factor, and has been implicated more generally in the precipitation of athero-thrombotic events[6]. Thus, rHDL infusions could complement existing treatments that directly target platelets or clotting factors. rHDL infusions may exert multiple beneficial effects in the setting of acute coronary syndromes, including removal of cholesterol and suppression of inflammation in plaques, suppression of excessive myeloid cell production and extramedullary hematopoiesis, as well as limitation of the overproduction of platelets[59,60]. Finally, while rHDL preparation and infusion as a chronic therapy remains challenging, our findings with Tolimidone suggests the pathway HDL activates to limit platelet production could be simulated by LYN kinase activators.

Online Methods

Mice and treatments

The Institutional Animal Care and Use Committee of Columbia University approved all the mouse studies. *Abcg4*$^{-/-}$, *Abcg1*$^{-/-}$ *Abca1*$^{-/-}$, and *Abcg1*$^{-/-}$ mice were created as described[14,48] and used in this study. *Abcg4*$^{-/-}$ mice have been backcrossed onto C57BL6/J mice for more than 10 generations. WT (C57BL/6J) and *Ldlr*$^{-/-}$ (B6.129S7-*Ldlrtm1Her)* were obtained from The Jackson Laboratory (Bar Harbor, Maine). For BM transplantation studies, BM from WT, *Abcg4*$^{-/-}$, *Abcg1*$^{-/-}$ *Abca1*$^{-/-}$, or *Abcg1*$^{-/-}$ mice was transplanted into WT or *Ldlr*$^{-/-}$ recipient mice as described. For atherosclerosis studies, the BM

transplanted recipient mice were fed a Western diet (TD88137; Harlan Teklad) for the indicated period of time. BM specific retroviral expression of murine MPL(W515L) was established as described[43], using WT C57BL6/J mice as the recipient and WT C57BL6/J or *Abcg4*$^{-/-}$ mice as the BM donor. Where indicated, vehicle (saline), rHDL, or TPO (R&D Systems) was injected at the indicted dose into the mice via the tail vein. The rHDL (CSL-111) was provided by CSL Behring AG, Bern, Switzerland; CSL-111 is comprised of human apoA-I and phosphatidylcholine from soy bean in a ratio of 1:150. All patients gave their informed consent to the study, which was approved by the Human Ethics Committee of the Alfred Hospital and conducted in accordance with the principles of the Declaration of Helsinki 2000.

Femur and tibia of *Lyn*$^{-/-}$ mice used to prepare *Lyn*$^{-/-}$ BM cells were kindly provided by Dr. Anthony L. DeFranco of University of California, San Francisco. The mice were created as described[61] and backcrossed at least 15 generations onto C57BL/6 background.

Histochemistry

Tissues and proximal aortas were serially paraffin sectioned and stained with H&E for morphological analysis as described[48]. Aortic lesion size of each animal was calculated as the mean of lesion areas in 5 sections from the same mouse. Bone samples were decalcified with EDTA solution prior to cryosectioning. Von Willibrand Factor antibody (Dako, Catalog # A0082) was used to stain MKs. Lac-Z staining of frozen sections of mouse bone, spleen or proximal aorta was carried out using β-Galactosidase Staining Kit (Cell Signaling Technology, Danvers, MA).

Complete blood count (CBC)

CBCs were quantified using whole blood collected from the tail bleeding. FORCYTE Veterinary Hematology Analyzer (Oxford Science, Inc.) was used for the analysis.

Plasma and cellular lipids

Plasma lipoprotein cholesterol and triglyceride levels were determined by colorimetric enzymatic assays, using the assay kits from Wako Diagnostics (Japan). Platelets were isolated from platelets-rich plasma, which was prepared from a low-speed spin of EDTA-treated mouse plasma, and platelet cholesterol content was measured by gas chromatography following lipid extraction.

Cholesterol efflux

For platelet cholesterol efflux, platelets were isolated from platelet-rich plasma by centrifugation at ~3500 rpm for 10 minutes in an Eppendorf centrifuge. The platelet-rich plasma was prepared from a low-speed spin of EDTA-treated mouse plasma. The isolated platelets were resuspended in DMEM cell culture media plus 0.2% bovine serum albumin. Cyclodexrin/cholesterol complexes containing [^{3}H]cholesterol was added to the final concentration of ~ 3 mM CD, and ~ 1 μCi [^{3}H]cholesterol/ml and the mixture was incubated at 37°C for 30 minutes. The labeled platelets were then washed three times with the same medium by brief spin and resuspension. HDL was then added to initiate the cholesterol

efflux and allowed to proceed for the time period as indicated. Cholesterol efflux was determined as percentage efflux (count of supernatant/total count ×100%).

To determine cholesterol efflux from MkPs to HDL, we labeled total BM cells by incubation with 0.03 mM methyl-β-cyclodextrin/BODIPY-cholesterol (molar ratio CD:cholesterol: BODIPY-cholesterol 40:0.8:0.2; Avanti Polar Lipids – Alabama, USA) in IMDM media plus 0.2% BSA at 37°C, 5% CO_2 for 30 minutes. The cells were washed three times with fresh IMDM media by brief spin and resuspension. CD or rHDL was then added to the cell suspension at the indicated concentration to initiate the efflux for the indicated period of time. The efflux was stopped by a brief spin and removal of the acceptors. The samples treated without CD or rHDL were used as the baseline for efflux. To assess BODIPY-cholesterol content in MkPs, the cell suspension was stained with a cocktail of lineage markers (Sca1, CD127, CD45R, CD19, CD11b, CD3e, TER-119, CD2, CD8, CD4, and Ly-6C/G; all APC; eBioscience) and progenitor cell markers, ckit, CD16/CD32 (FcγRII/III), CD34, CD41. MkPs were identified as lineage^{-}, ckit^{+}, CD16/CD32^{lo}, CD34^{lo} and CD41^{+} and the mean fluorescence intensity (MFI) of BODIPY-cholesterol from MkPs was measured by flow cytometry (LSRII, BD Biosciences) to assess BODIPY-cholesterol content in MkPs or cholesterol efflux (1-remaining MFI/baseline MFI×100%).

Flow cytometry based proliferation studies

Blood leukocytes and BM HSPCs were stained and analyzed or sorted as described[49]. Briefly, BM cells from the mouse femurs and tibias were stained with a cocktail of antibodies to lineage committed cells (CD45R, CD19, CD11b, CD3e, TER-119, CD2, CD8, CD4, Ly-6C/G: All FITC, eBioscience), antibodies to Sca1 (Pacific Blue) and ckit (APC Cy7) to identify HSPC populations and LSK (lin−, Sac1+ and ckit+) cells, and antibodies to CD16/CD32 (FcγRII/III), CD34 to separate CMP (lin−, Sca1−, ckit+, CD34int, FcγRII/IIIint), GMP (lin−, Sca1−, ckit+, CD34int, FcγRII/IIIhi), MEP (lin−, Sca1−, ckit+, CD34lo, FcγRII/IIIlo). For DNA content analysis (G2M phase), BM cells were fixed, and stained with DAPI (Invitrogen) prior to flow cytometry analysis. To determine in vivo cell proliferation, EdU (Invitrogen) was injected into mice via the tail vein 24 hours prior to being sacrificed. Cells were immunostained as described above in preparation for flow cytometry. Cells were then fixed and permeabilized using 0.01% saponin (w/v; Fluka) and 1% FCS (v/v) in IC fixation buffer (eBiosciences) for 30 minutes. Cells were then washed and stained with Alexa Fluor–conjugated azides using the Click-iT system (Invitrogen). Proliferation was quantified as percentage of EdU^{+} cells by flow cytometry.

Quantification of reticulated platelets

Undiluted EDTA-anticoagulated blood (5 μl) was mixed with a PE-anti-CD41 antibody and the fluorescent DNA-dye thiazole orange (TO) (final concentration 1μg/ml) and incubated at room temperature for 20 minutes. Samples were then fixed by adding 1 ml of 1% formaldehyde in PBS. Data acquisition using logarithmic amplification of lightscatter and fluorescence signals was performed. PE-positive cells were gated in a TO versus PE dot plot.

Quantitative real time RT-PCR (q-PCR)

RNA extraction, cDNA synthesis, and q-PCR of HSPCs were performed as described[49]. The quality of RNA samples was determined using Agilent 2100 Bioanalyzer and RNA 6000 LabChip. The primer sequences used for q-PCR are shown in Table S1.

Megakaryocyte Colony Forming Unit assay

Primary BM HSPC cells obtained by FACS were plated in methylcellulose-based media (5000 cells/assay) containing TPO (50ng/mL), IL-6 (20ng/mL), and IL-3 (10 ng/mL) and incubated for 8 days according to manufacturer's protocol (Megacult-C, Stemcell Technologies). Cultures were fixed and the MK colonies visualized by staining for acethylcholinesterase activity. Nuclei were counterstained with Harris' hematoxylin. Colonies containing more than 3 megakaryocytes were scored as CFU-Mk.

Anti-ABCG4 antibody

The rabbit anti-ABCG4 antibody was custom made by Pacific Immunology (CA, USA) against a synthetic ABCG4 peptide (KKVENHITEAQRFSHLPKR). The mono-specific anti-peptide antibodies were purified using a peptide-affinity column. The specificity of the antibody for ABCG4 protein was assessed by immunofluorescence microscopy which showed specific immunofluorescence signals in HEK293 cells expressing ABCG4 but not HEK293 cells transfected with mock vectors (not shown).

Rabbit polyclonal anti-c-MPL antibody was kindly provided by Dr. Wei Tong of University of Pennsylvania and the specificity of the antibody against cell surface c-MPL in flow cytometry has been reported previously[62,63].

Neutrophil and monocyte – platelet aggregates

Blood was collected via the tail vein into EDTA lined tubes on ice to prevent leukocyte activation. RBCs were lysed and the washed cells were then stained with CD45, CD115, Gr1 (Ly6-C/G), CD11b and CD41 for 30mins on ice. The cells were carefully washed, resuspended in FACS buffer and run on the LSRII to detect leukocyte platelet interactions and leukocyte activation. Viable cells were selected based on forward and side scatter characteristics and then $CD45^+$ leukocytes were selected. Ly6-C^{hi} monocyte platelet aggregates were identified as $CD115^+Gr1^{hi}$ (Ly6-C^{hi}) $CD41^+$. Neutrophils platelet aggregates were identified as $CD115^-Gr1^+$ (Ly6-G^+) $CD41^+$. Platelet dependent activation of Ly6-C^{hi} monocytes and neutrophils was measured as CD11b MFI after subtracting the expression of CD11b on Ly6-C^{hi} or neutrophils, which were not interacting with platelets.

Platelet derived microparticles

Equal amounts of mouse plasma (20μL) was diluted with HEPES binding buffer (80μL) and then incubated with annexin V and anti-CD41. Equal amounts of 1μm beads (Invitrogen) were added to the sample, which was then run on an LSR-II. Platelet derived microparticles were detected as particles less than 1μm in size that stained positive for CD41 and annexin V. A stopping gate was placed over the beads, to ensure accurate counting in each sample. Data was converted to number of microparticles per 1μL of whole blood.

$FeCl_3$ induced carotid artery thrombosis

Mice were anesthetized and a cervical incision was made to expose the common carotid artery. A miniature Doppler flow probe (TS420 transit-time perivascular flowmeter, Transonic Systems Inc.) was placed on the carotid artery to monitor blood flow. The injury to the artery was induced by a piece of Whatman paper (2×2mm) saturated with 5% $FeCl_3$. The time to the cessation of the blood flow was recorded as occlusion time.

Ex vivo flow chamber assay

Heparin (5U/ml) anticoagulated whole blood was incubated with 1μM of fluorescent dye DiOC6 (Sigma, St. Louis. Mo, USA) for 10 minutes at 37°C. Then, the fluorescently labeled whole blood was perfused over the collagen coated glass cover surface (microcapillary glass tube coated with 100μm/mL Horm collagen (Nycomed) overnight) at a controlled shear rate ($1800s^{-1}$) using a syringe pump for 3 minutes. Adherent platelets and aggregates in the chamber were washed and examined under inverted fluorescent microscope and pictures of adhered platelets were recorded for analysis. Surface coverage was calculated using ImageJ.

c-MPL expression

Detection of c-MPL from *in vivo* and *in vitro* experiments was performed as follows. After harvesting BM progenitor cells, RBCs were lysed and the cells were then resuspended in FACS buffer. Cells were then stained with a cocktail of lineage markers to allow negative selection of BM progenitor cells (Sca1, CD127, CD45R, CD19, CD11b, CD3e, TER-119, CD2, CD8, CD4, and Ly-6C/G; all FITC; eBioscience) and progenitor cell markers, ckit, CD16/CD32 (FcγRII/III), CD34, CD41 and c-MPL or isotype control and allowed to stain on ice for 30mins. Cells were then washed and stained with a fluorescently conjugated secondary anti-rabbit antibody to detect the anti-c-MPL for a further 30mins on ice. After this the cells were washed, resuspended in FACS buffer and run on the LSRII. MEPs were identified as $lin^{-}ckit^{+}CD16/CD32^{lo}CD34^{lo}CD41^{-}$, while MkPs were identified as $lin^{-}ckit^{+}CD16/CD32^{lo}CD34^{lo}CD41^{+}$.

Expression of c-MPL on late stage megakaryocyte was achieved by staining BM cells with a cocktail of lineage markers (Sca1, CD127, CD45R, CD19, CD3e, TER-119, CD2, CD8 and Ly6-C/G –all FITC), CD41 and c-Mpl or isotype control as above. After staining with the antibodies the BM cells were then fixed and permeabilized using BD cytofix/perm buffer for 20mins on ice, followed by washing with BD cytofix/perm wash buffer. Cells were the resuspended in FACS buffer containing propidium iodide to detect megakaryocyte ploidy. Expression of c-MPL was measured on total and late stage megakaryocytes (defined at 32N and 64N).

Expression of c-MPL on platelets was carried out by obtaining PRP and staining with CD41 and c-MPL as outlined above.

The expression of c-MPL was quantified in these respective populations by MFI, normalized to the isotype control.

c-Cbl phosphorylation

BM progenitor cells were stimulated with TPO at the indicated concentration for the specified period of time at 37°C and then immediately diluted with ice-cold buffer and placed on ice to prevent further changes in phosphorylation. Cells were then centrifuged and the pellet resuspended in BD fix buffer (BD Biosciences) for 10mins on ice. The cells were washed with BD flow cytometry staining buffer, centrifuged and then resuspended in BD cytofix/perm buffer III for 20 mins. After this the cells were washed and resuspended in BD staining buffer and incubated with lineage (Sca1, CD127, CD45R, CD19, CD11b, CD3e, TER-119, CD2, CD8, CD4, and Ly-6G; all FITC; eBioscience) and progenitor cell markers, ckit, CD16/CD32 (FcγRII/III), CD34, CD41 and anti-phospho-c-Cbl (Y700human/Y698mouse; BD biosciences) or an isotype control for 30mins on ice. The cells were then washed, resuspended in FACS buffer and run on an LSRII. Phosphorylated c-Cbl was normalized against isotype control staining.

Immunofluorescence confocal microscopy

MkPs collected by FACS from WT or *Abcg4*$^{-/-}$ BM cells were forced to attach to glass slides by a brief spin in Cytospin. The cells were then fixed with 2% paraformaldehyde, permeabilized with 1% Triton X-100 in PBS for 1 minute and incubated with 4% BSA in PBS plus 0.1% saponin to block the non-specific binding sites. The diluted primary antibodies against ABCG4 or cellular organelle markers (58K Golgi protein antibody, Novus Biologicals; TGN38 antibody, BD Biosciences; c-MPL antibody, Sigma-Aldrich; Lamp2 antibody, Novus Biologicals) were then added to incubate with the cells. After washing, the fluorescent secondary antibodies were added. Where indicated, the washed cells were counterstained with or without DAPI and examined with fluorescence confocal microscope.

Statistics

For aortic morphometric atherosclerotic lesion quantification and analysis, two-way ANOVA was used. For comparison of one group with another, for instance the c-Cbl phosphorylation time course as shown in Fig. 4A, t test was used. For comparison of various treatments on different genotypes, one-way ANOVA was used.

Supplementary Material

Refer to Web version on PubMed Central for supplementary material.

Acknowledgments

A.J.M was supported by a post-doctoral fellowship from the American Heart Association (AHA; 12POST11890019).

References

1. Labarthe DR, Dunbar SB. Global cardiovascular health promotion and disease prevention: 2011 and beyond. Circulation. 2012; 125:2667–2676. [PubMed: 22644371]
2. Libby P, Ridker PM, Hansson GK. Progress and challenges in translating the biology of atherosclerosis. Nature. 2011; 473:317–325. [PubMed: 21593864]

3. Koenen RR, et al. Disrupting functional interactions between platelet chemokines inhibits atherosclerosis in hyperlipidemic mice. Nature medicine. 2009; 15:97–103.
4. Huo Y, et al. Circulating activated platelets exacerbate atherosclerosis in mice deficient in apolipoprotein E. Nature medicine. 2003; 9:61–67.
5. Coller BS. Historical perspective and future directions in platelet research. J Thromb Haemost. 2011; 9 (Suppl 1):374–395. [PubMed: 21781274]
6. Martin JF, Kristensen SD, Mathur A, Grove EL, Choudry FA. The causal role of megakaryocyte-platelet hyperactivity in acute coronary syndromes. Nature reviews Cardiology. 2012; 9:658–670. [PubMed: 22987055]
7. Trip MD, Cats VM, van Capelle FJ, Vreeken J. Platelet hyperreactivity and prognosis in survivors of myocardial infarction. N Engl J Med. 1990; 322:1549–1554. [PubMed: 2336086]
8. Hasselbalch HC. Perspectives on chronic inflammation in essential thrombocythemia, polycythemia vera, and myelofibrosis. Blood. 2012
9. Tefferi A, Vainchenker W. Myeloproliferative neoplasms: molecular pathophysiology, essential clinical understanding, and treatment strategies. J Clin Oncol. 2011; 29:573–582. [PubMed: 21220604]
10. Steinberg D. The statins in preventive cardiology. N Engl J Med. 2008; 359:1426–1427. [PubMed: 18832243]
11. Tall AR, Yvan-Charvet L, Terasaka N, Pagler T, Wang N. HDL, ABC transporters, and cholesterol efflux: implications for the treatment of atherosclerosis. Cell Metab. 2008; 7:365–375. [PubMed: 18460328]
12. Pathansali R, Smith N, Bath P. Altered megakaryocyte-platelet haemostatic axis in hypercholesterolaemia. Platelets. 2001; 12:292–297. [PubMed: 11487381]
13. Wang N, Lan D, Chen W, Matsuura F, Tall AR. ATP-binding cassette transporters G1 and G4 mediate cellular cholesterol efflux to high-density lipoproteins. Proceedings of the National Academy of Sciences of the United States of America. 2004; 101:9774–9779. [PubMed: 15210959]
14. Wang N, Ranalletta M, Matsuura F, Peng F, Tall AR. LXR-induced redistribution of ABCG1 to plasma membrane in macrophages enhances cholesterol mass efflux to HDL. Arteriosclerosis, thrombosis, and vascular biology. 2006; 26:1310–1316.
15. Annilo T, et al. Human and mouse orthologs of a new ATP-binding cassette gene, ABCG4. Cytogenetics and cell genetics. 2001; 94:196–201. [PubMed: 11856881]
16. Bojanic DD, et al. Differential expression and function of ABCG1 and ABCG4 during development and aging. Journal of lipid research. 51:169–181. [PubMed: 19633360]
17. Ranalletta M, et al. Decreased atherosclerosis in low-density lipoprotein receptor knockout mice transplanted with Abcg1−/− bone marrow. Arteriosclerosis, thrombosis, and vascular biology. 2006; 26:2308–2315.
18. Meurs I, et al. The effect of ABCG1 deficiency on atherosclerotic lesion development in LDL receptor knockout mice depends on the stage of atherogenesis. Atherosclerosis. 2012; 221:41–47. [PubMed: 22196936]
19. Mazzone A, et al. Increased expression of neutrophil and monocyte adhesion molecules in unstable coronary artery disease. Circulation. 1993; 88:358–363. [PubMed: 8101771]
20. Mause SF, von Hundelshausen P, Zernecke A, Koenen RR, Weber C. Platelet microparticles: a transcellular delivery system for RANTES promoting monocyte recruitment on endothelium. Arteriosclerosis, thrombosis, and vascular biology. 2005; 25:1512–1518.
21. Guthikonda S, et al. Role of reticulated platelets and platelet size heterogeneity on platelet activity after dual antiplatelet therapy with aspirin and clopidogrel in patients with stable coronary artery disease. Journal of the American College of Cardiology. 2008; 52:743–749. [PubMed: 18718422]
22. Lakkis N, et al. Reticulated platelets in acute coronary syndrome: a marker of platelet activity. Journal of the American College of Cardiology. 2004; 44:2091–2093. [PubMed: 15542299]
23. Stohlawetz P, et al. Measurement of the levels of reticulated platelets after plateletpheresis to monitor activity of thrombopoiesis. Transfusion. 1998; 38:454–458. [PubMed: 9633558]
24. Nofer JR, van Eck M. HDL scavenger receptor class B type I and platelet function. Curr Opin Lipidol. 2011; 22:277–282. [PubMed: 21537173]

25. Villmow T, Kemkes-Matthes B, Matzdorff AC. Markers of platelet activation and platelet-leukocyte interaction in patients with myeloproliferative syndromes. Thromb Res. 2002; 108:139–145. [PubMed: 12590950]
26. Pikman Y, et al. MPLW515L is a novel somatic activating mutation in myelofibrosis with myeloid metaplasia. PLoS Med. 2006; 3:e270. [PubMed: 16834459]
27. Frontelo P, et al. Novel role for EKLF in megakaryocyte lineage commitment. Blood. 2007; 110:3871–3880. [PubMed: 17715392]
28. Hitchcock IS, Chen MM, King JR, Kaushansky K. YRRL motifs in the cytoplasmic domain of the thrombopoietin receptor regulate receptor internalization and degradation. Blood. 2008; 112:2222–2231. [PubMed: 18487512]
29. Tiedt R, et al. Pronounced thrombocytosis in transgenic mice expressing reduced levels of Mpl in platelets and terminally differentiated megakaryocytes. Blood. 2009; 113:1768–1777. [PubMed: 18845793]
30. Kelemen E, Lehoczky D, Jakab K, Batai A, Vargha P. Responses to single-dose thrombopoietin decrease with higher platelet counts in mice. Acta haematologica. 1999; 101:41–45. [PubMed: 10085437]
31. Brown MS, Goldstein JL. Cholesterol feedback: from Schoenheimer's bottle to Scap's MELADL. Journal of lipid research. 2009; 50 (Suppl):S15–27. [PubMed: 18974038]
32. Lingwood D, Simons K. Lipid rafts as a membrane-organizing principle. Science. 2010; 327:46–50. [PubMed: 20044567]
33. Saur SJ, Sangkhae V, Geddis AE, Kaushansky K, Hitchcock IS. Ubiquitination and degradation of the thrombopoietin receptor c-Mpl. Blood. 2010; 115:1254–1263. [PubMed: 19880496]
34. Nadeau S, et al. Oncogenic Signaling by Leukemia-Associated Mutant Cbl Proteins. Biochem Anal Biochem. 2012; S6–001:1–7.
35. Hunter S, Burton EA, Wu SC, Anderson SM. Fyn associates with Cbl and phosphorylates tyrosine 731 in Cbl, a binding site for phosphatidylinositol 3-kinase. The Journal of biological chemistry. 1999; 274:2097–2106. [PubMed: 9890970]
36. Blake RA, et al. SU6656, a selective src family kinase inhibitor, used to probe growth factor signaling. Mol Cell Biol. 2000; 20:9018–9027. [PubMed: 11074000]
37. Lannutti BJ, Shim MH, Blake N, Reems JA, Drachman JG. Identification and activation of Src family kinases in primary megakaryocytes. Experimental hematology. 2003; 31:1268–1274. [PubMed: 14662334]
38. Oneyama C, et al. Transforming potential of Src family kinases is limited by the cholesterol-enriched membrane microdomain. Mol Cell Biol. 2009; 29:6462–6472. [PubMed: 19822664]
39. Lannutti BJ, Minear J, Blake N, Drachman JG. Increased megakaryocytopoiesis in Lyn-deficient mice. Oncogene. 2006; 25:3316–3324. [PubMed: 16418722]
40. Ingley E, et al. Lyn deficiency reduces GATA-1, EKLF and STAT5, and induces extramedullary stress erythropoiesis. Oncogene. 2005; 24:336–343. [PubMed: 15516974]
41. Saporito MS, Ochman AR, Lipinski CA, Handler JA, Reaume AG. MLR-1023 is a potent and selective allosteric activator of Lyn kinase in vitro that improves glucose tolerance in vivo. J Pharmacol Exp Ther. 2012; 342:15–22. [PubMed: 22473614]
42. Tardif JC, et al. Effects of reconstituted high-density lipoprotein infusions on coronary atherosclerosis: a randomized controlled trial. JAMA : the journal of the American Medical Association. 2007; 297:1675–1682. [PubMed: 17387133]
43. Koppikar P, et al. Efficacy of the JAK2 inhibitor INCB16562 in a murine model of MPLW515L-induced thrombocytosis and myelofibrosis. Blood. 2010; 115:2919–2927. [PubMed: 20154217]
44. Marty C, et al. Ligand-independent thrombopoietin mutant receptor requires cell surface localization for endogenous activity. The Journal of biological chemistry. 2009; 284:11781–11791. [PubMed: 19261614]
45. Shaw JA, et al. Infusion of reconstituted high-density lipoprotein leads to acute changes in human atherosclerotic plaque. Circulation research. 2008; 103:1084–1091. [PubMed: 18832751]
46. Brown MS, Goldstein JL. Suppression of 3-hydroxy-3-methylglutaryl coenzyme A reductase activity and inhibition of growth of human fibroblasts by 7-ketocholesterol. The Journal of biological chemistry. 1974; 249:7306–7314. [PubMed: 4436312]

47. Brown MS, Goldstein JL. Multivalent feedback regulation of HMG CoA reductase, a control mechanism coordinating isoprenoid synthesis and cell growth. Journal of lipid research. 1980; 21:505–517. [PubMed: 6995544]
48. Yvan-Charvet L, et al. ATP-binding cassette transporters and HDL suppress hematopoietic stem cell proliferation. Science. 2010; 328:1689–1693. [PubMed: 20488992]
49. Murphy AJ, et al. ApoE regulates hematopoietic stem cell proliferation, monocytosis, and monocyte accumulation in atherosclerotic lesions in mice. The Journal of clinical investigation. 2011; 121:4138–4149. [PubMed: 21968112]
50. Bensinger SJ, et al. LXR signaling couples sterol metabolism to proliferation in the acquired immune response. Cell. 2008; 134:97–111. [PubMed: 18614014]
51. Armstrong AJ, Gebre AK, Parks JS, Hedrick CC. ATP-binding cassette transporter G1 negatively regulates thymocyte and peripheral lymphocyte proliferation. J Immunol. 2010; 184:173–183. [PubMed: 19949102]
52. Kovarova M, et al. Structure-function analysis of Lyn kinase association with lipid rafts and initiation of early signaling events after Fcepsilon receptor I aggregation. Mol Cell Biol. 2001; 21:8318–8328. [PubMed: 11713268]
53. Gieger C, et al. New gene functions in megakaryopoiesis and platelet formation. Nature. 2011; 480:201–208. [PubMed: 22139419]
54. Barter PJ, et al. Effects of torcetrapib in patients at high risk for coronary events. N Engl J Med. 2007; 357:2109–2122. [PubMed: 17984165]
55. Boden WE, et al. Niacin in patients with low HDL cholesterol levels receiving intensive statin therapy. N Engl J Med. 2011; 365:2255–2267. [PubMed: 22085343]
56. Rader DJ, Tall AR. The not-so-simple HDL story: Is it time to revise the HDL cholesterol hypothesis? Nature medicine. 2012; 18:1344–1346.
57. Verstovsek S, et al. Safety and efficacy of INCB018424, a JAK1 and JAK2 inhibitor, in myelofibrosis. N Engl J Med. 2010; 363:1117–1127. [PubMed: 20843246]
58. Wolanskyj AP, Schwager SM, McClure RF, Larson DR, Tefferi A. Essential thrombocythemia beyond the first decade: life expectancy, long-term complication rates, and prognostic factors. Mayo Clinic proceedings Mayo Clinic. 2006; 81:159–166.
59. Dutta P, et al. Myocardial infarction accelerates atherosclerosis. Nature. 2012; 487:325–329. [PubMed: 22763456]
60. Tall AR, Yvan-Charvet L, Westerterp M, Murphy AJ. Cholesterol efflux: a novel regulator of myelopoiesis and atherogenesis. Arteriosclerosis, thrombosis, and vascular biology. 2012; 32:2547–2552.
61. Chan VW, Meng F, Soriano P, DeFranco AL, Lowell CA. Characterization of the B lymphocyte populations in Lyn-deficient mice and the role of Lyn in signal initiation and down-regulation. Immunity. 1997; 7:69–81. [PubMed: 9252121]
62. Tong W, Ibarra YM, Lodish HF. Signals emanating from the membrane proximal region of the thrombopoietin receptor (mpl) support hematopoietic stem cell self-renewal. Experimental hematology. 2007; 35:1447–1455. [PubMed: 17637498]
63. Bersenev A, Wu C, Balcerek J, Tong W. Lnk controls mouse hematopoietic stem cell self-renewal and quiescence through direct interactions with JAK2. The Journal of clinical investigation. 2008; 118:2832–2844. [PubMed: 18618018]

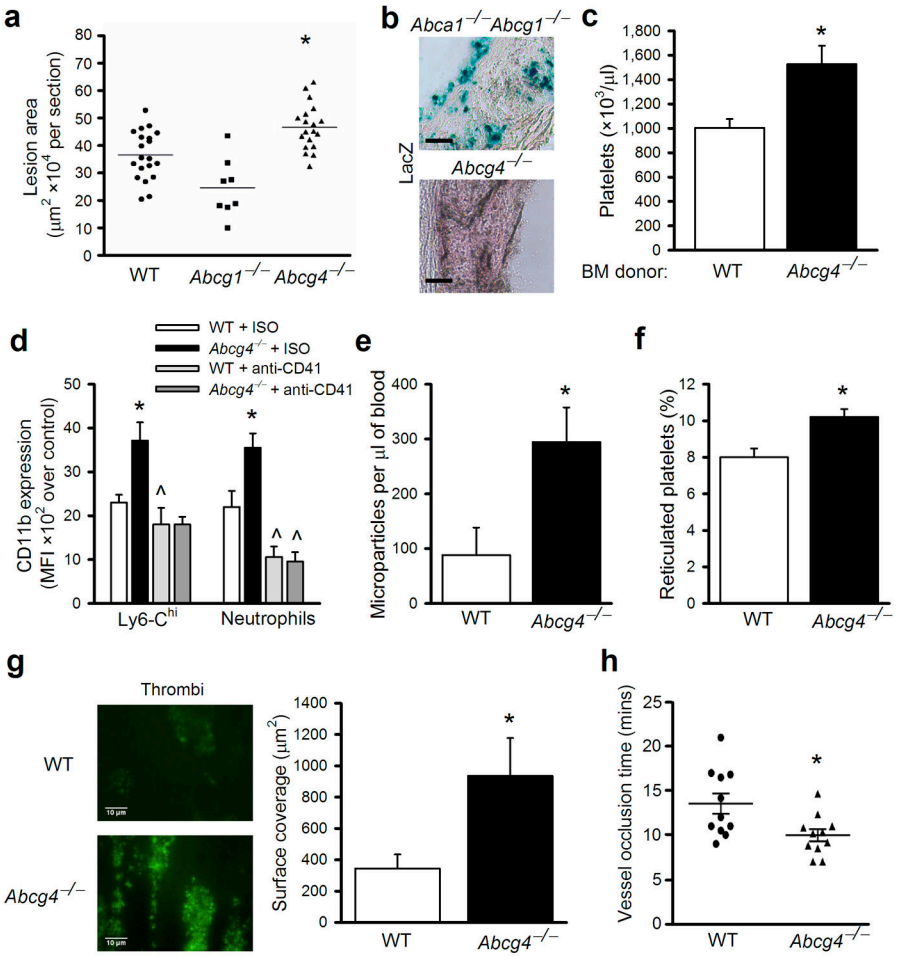

Figure 1.

BM ABCG4 deficiency increases platelet count and accelerates atherosclerosis and thrombosis. *Ldlr*$^{-/-}$ mice were transplanted with donor BM cells from WT, *Abcg4*$^{-/-}$, *Abcg1*$^{-/-}$ or *Abca1*$^{-/-}$*Abcg1*$^{-/-}$ mice and fed a WTD diet for 12 weeks. (**a**) Quantification of proximal aortic root lesion area (individual and mean) by morphometric analysis of H&E-stained sections. Scale Bar=50μm. (**b**) Representative of LacZ stained proximal aortas from mice receiving *Abca1*$^{-/-}$*Abcg1*$^{-/-}$ or *Abcg4*$^{-/-}$ BM. Original magnification 40x. (**c**) Platelet counts from mice receiving WT or *Abcg4*$^{-/-}$ BM. Data are means ± SEM (n=12), representative result of 4 independent studies. (**d**) Cell surface CD11b levels of platelet-associated Ly6C^{hi} monocytes or neutrophils in WTD-fed *Ldlr*$^{-/-}$ mice transplanted with WT or *Abcg4*$^{-/-}$ BM cells. (**e**) Plasma platelet-derived microparticle and (**f**) percentage reticulated platelets levels in WTD-fed *Ldlr*$^{-/-}$ recipient mice. (**g**) Microthrombi formation on collagen under shear flow with blood from WTD-fed *Ldlr*$^{-/-}$ recipient mice. (**h**) $FeCl_3$ induced carotid artery thrombosis in vivo in WTD-fed *Ldlr*$^{-/-}$ recipient mice. Data are means ± SEM, * P<0.05 between genotypes. ^P<0.05 between the basal and treatment.

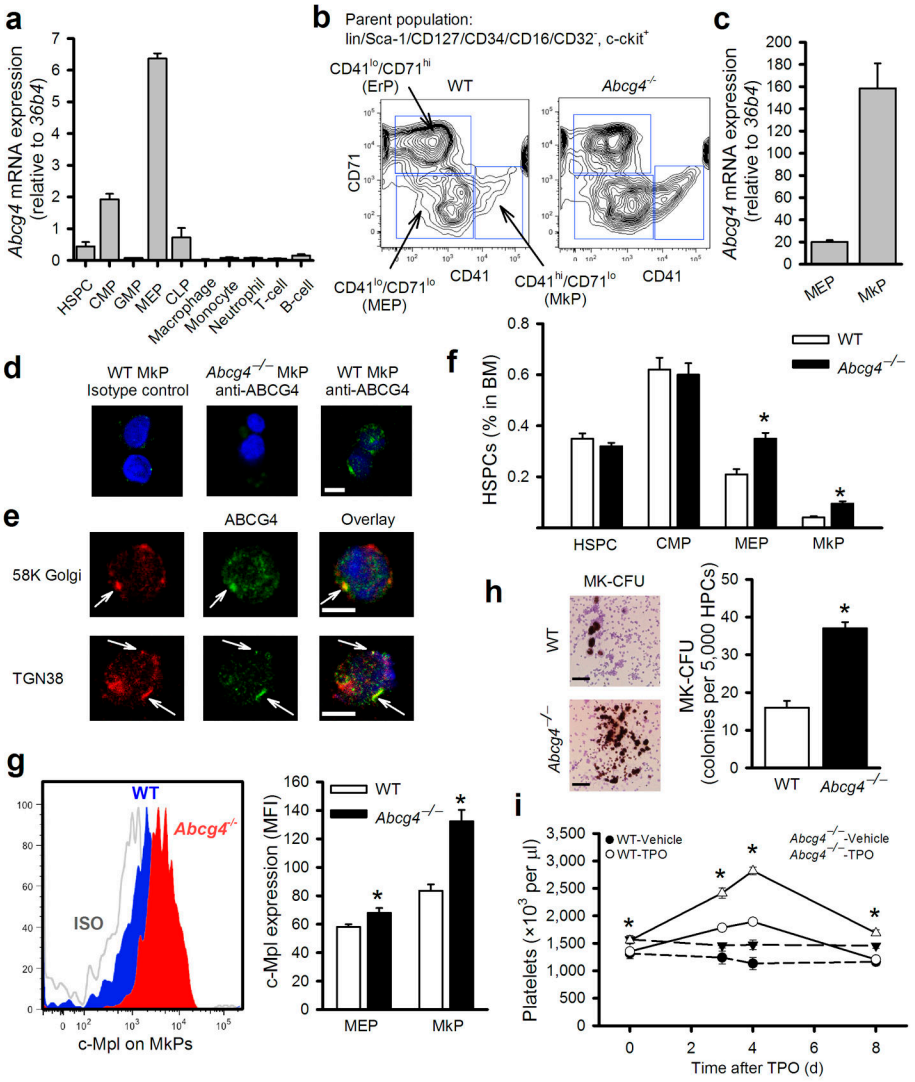

Figure 2.

Abcg4 is highly expressed in MkPs, regulating megakaryopoiesis and c-MPL levels. (**a**) *Abcg4* mRNA expression in various types of BM and peripheral white blood cells in WT mice determined by q-PCR. (n=5). (**b**) Flow cytometry analysis of $CD41^{lo}/CD71^{+}$ (ErP), $CD41^{+}/CD71^{lo}$ (MkP) and $CD41^{lo}/CD71^{lo}$ (MEP) cells from the parent MEP population of Fig. S4. (**c**) *Abcg4* expression in MEPs and MkPs as assessed by quantitative RT-PCR. (**d**) ABCG4 protein expression in MkPs assessed by immunofluorescence confocal microscopy. The cells were stained with isotype control or anti-ABCG4 (green) and DAPI (nuclei, blue). Scale bar=5μm. (**e**) Confocal microscopy of WT MkPs immunostained with anti-ABCG4 (green), anti-58K Golgi or anti-TGN38 (red) and DAPI (blue). Scale bar=5μm. (**f**) Quantification of BM cell populations and (**g**) cell surface c-MPL levels of $Ldlr^{-/-}$ recipient mice fed WTD for 12 weeks (n=5). (**h**) MK-CFU assay using HPCs harvested by FACS from WT or $Abcg4^{-/-}$ mice. Scale bar=50μm. (**i**) Platelet count in the WT and $Abcg4^{-/-}$ mice (n=5) receiving a single dose of TPO (50μg/kg BW) or the vehicle control. Data are means ± SEM, *P<0.05 WT versus $Abcg4^{-/-}$ groups and ^P<0.05 for treatment effect.

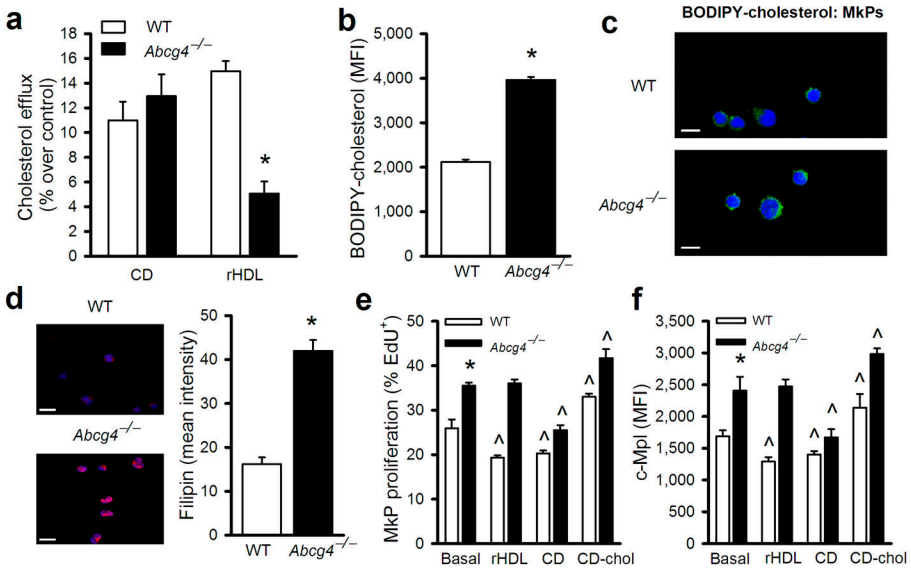

Figure 3.

ABCG4 deficiency decreases cholesterol efflux, increases membrane cholesterol content and proliferation of MkPs. (**a**) Bodipy-cholesterol efflux from WT or *Abcg4*$^{-/-}$ MkPs to CD (2 mM) or rHDL (20 μg /ml) for 2 hours (n=4). (**b**) Bodipy-cholesterol levels in WT or *Abcg4*$^{-/-}$ MkPs following CD/Bodipy-cholesterol loading (n=4). (**c**) Confocal fluorescence microscopy of MkPs from WT and *Abcg4*$^{-/-}$ mice incubated with CD/Bodipy-cholesterol (green) and TO-PRO-3 (nuclei, blue). Scale bar=5μm. (**d**) Confocal microscopy of WT and *Abcg4*$^{-/-}$ MkPs stained with fillipin (red) and DAPI (blue) and quantification. Scale bar=10 μm. (**e**) EdU incorporation into and (**f**) cell surface c-MPL of WT or *Abcg4*$^{-/-}$ MkPs were determined by flow cytometry (n=4). Data are means ± SEM, *P<0.05 WT versus *Abcg4*$^{-/-}$ groups and $^{\wedge}$P<0.05 for treatment effect.

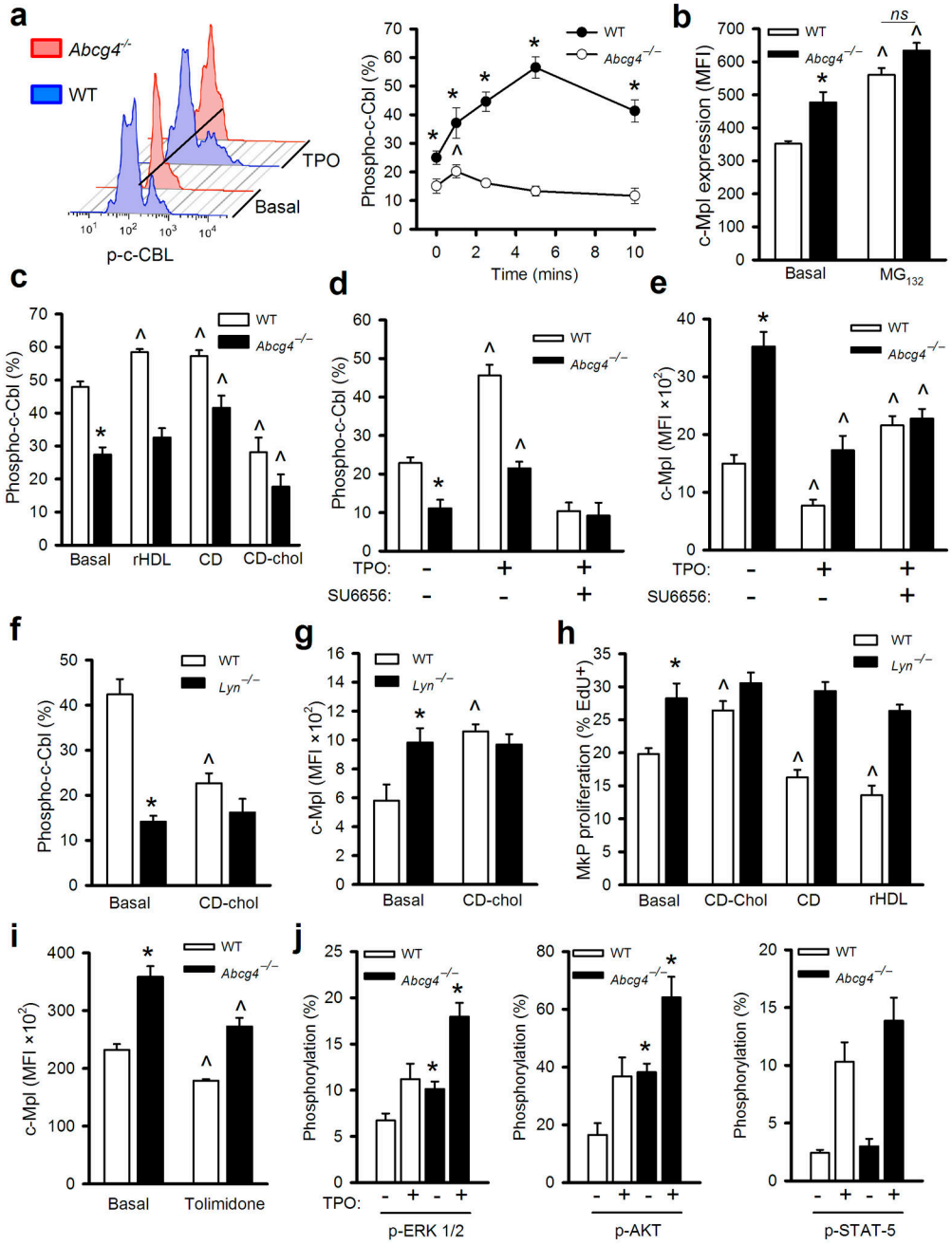

Figure 4.

Increased MkP c-MPL and proliferation in ABCG4 deficiency involves altered activity of c-CBL and LYN. Shown are results all from WT, *Abcg4*$^{-/-}$ or *Lyn*$^{-/-}$ MkPs (n=4). (**a**) c-CBL phosphorylation in response to TPO was quantified by phosphor-flow cytometry. Representative histograms before and after 10 mins of TPO. (**b**) Cell surface c-MPL levels with or without MG132 treatment (10 μM) for 2 h in the presence of TPO. (**c**) c-CBL phosphorylation 5 min after TPO treatment with or without pretreatment with CD (3 mM), CD-chol (3 mM CD) for 30 min or rHDL (20 μg apoA-I/ml) for 2 hours. (**d**) c-CBL phosphorylation with or without 5 min TPO treatment or SU6656 pretreatment (10 μg/ml for

2 h). (**e**) Cell surface c-MPL levels on MkPs with or without TPO or SU6656 treatment for 2 h. (**f**) Tyrosine-phosphorylated c-CBL (5 min in response to TPO) or (**g**) cell surface c-MPL (2 h TPO treatment) with or without pretreatment with CD-chol (3 mM CD) for 30 min. (**h**) 16 h EdU incorporation in the presence of TPO and with or without CD (3 mM), CD-Chol (3 mM CD) pretreatment for 30 min or rHDL (20 μg/ml) for 16 h. (**i**) BM was isolated from WTD-fed BMT *Ldlr*$^{-/-}$ recipients and cell surface c-MPL levels quantified after treatment with or without the LYN activator Tolimidone (10 μM) in the presence of TPO for 2 hours. (**j**) p-ERK1/2, p-AKT and p-STAT-5 levels with or without TPO for 10 minutes. TPO was 30 ng/ml for all the assays shown. Data are means ± SEM, *P<0.05 WT vs *Abcg4*$^{-/-}$ TPO and $^{\wedge}$P<0.05 for treatment effect.

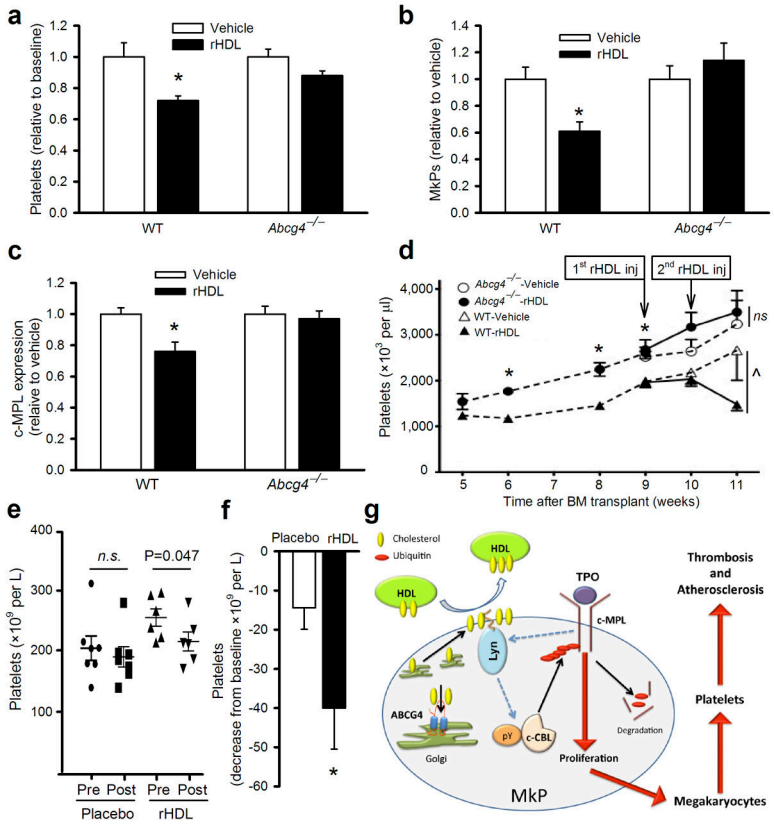

Figure 5.

rHDL suppresses platelet production in an ABCG4-dependent fashion in vivo. WTD-fed *Ldlr*$^{-/-}$ recipient mice (n=5) received a single infusion of vehicle or rHDL (100 mg apoA-I/kg BW). 5 days post infusion (**a**) platelet counts were determined using a hematology analyzer. Flow cytometry was used to determine (**b**) abundance of BM MkPs and (**c**) BM MkP c-MPL experssion. (**d**) WT mice were transplanted with donor BM cells from WT (n=10) or *Abcg4*$^{-/-}$mice (n=10), both transduced with *Mpl*^{W515L}. Platelet counts were monitored weekly and at 9 weeks post-transplant mice received two weekly infusions of rHDL (100mg apoA-I/kg BW) or vehicle as indicated (n=5 per subgroup). Data are means ± SEM, *P<0.05 WT versus *Abcg4*$^{-/-}$ and ^P<0.05 for treatment effect. (**e, f**) Patients with peripheral vascular disease received a single infusion of rHDL (80mg/kg BW) or placebo. (**e**) Platelet counts were measured pre- and 5 days post-infusion. (**f**) Data is presented as mean decrease in total platelets post-infusion (n=7/group). (**g**) Schematic model depicting the involvement of ABCG4 in the regulation of c-MPL levels.